Nanoscale

Accepted Manuscript

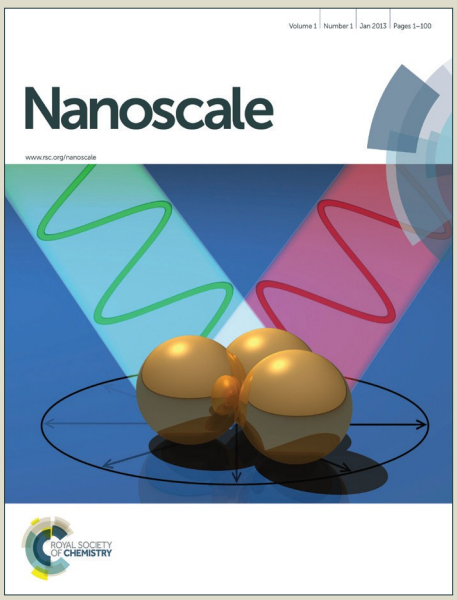

ROYAL SOCIETY OF CHEMISTRY

www.rsc.org/nanoscale

Journal Name

RSCPublishing

ARTICLE

Single Layer Nano Graphene Platelets Derived From Graphite Nanofibres

Cite this: DOI: 10.1039/x0xx00000x

Kai Huang,[a,b] Géraud Delport,[c] Lucile Orcin-Chaix,[c] Carlos Drummond,[a,b] Jean-Sebastien Lauret,[c] and Alain Penicaud*[a,b]

Received ooth January 2012,
Accepted ooth January 2012

DOI: 10.1039/x0xx00000x

www.rsc.org/

Solutions of calibrated nanographenides (negatively charged nanographenes) are obtained by dissolution of graphite nanofibre intercalation compounds (GNFICs). Deposits show homogeneous unfolded nanographene platelets of 1 to 2 layers thickness and 10 nm lateral size, evidenced by atomic force microscopy and Raman spectroscopy. Upon oxidation, nanographenide solutions exhibit strong photoluminescence.

Introduction

Graphene has received extensive attention for its potential applications as one of the few known two-dimensional materials, due to its intriguing electrical, mechanical, and chemical properties.[1-4] The procedures used to produce graphene include micromechanical cleavage,[1] chemical vapor deposition (CVD)[5,6] and thermal decomposition of SiC.[7] However, low-yield and/or high costs restrain their use for industrial scale applications. To overcome this limitation, many studies have explored liquid phase routes in the past years.[8-16] One of these studies consists in sonication-free, mild dissolution of graphite in organic solvents, by using graphite intercalation compounds (GICs), allowing the deposition of monolayer graphene on surfaces.[13-16] By inserting alkali metals into graphene layers, the π-π interactions between layers are replaced by electrostatic interactions. It has been shown that in suitable solvents, the entropic counter ion contribution drives the spontaneous dissolution of nanocarbon salts.[17] Thus, solutions of negatively charged graphene sheets, i.e. graphenides, can be obtained in polar solvents such as THF or NMP.[15,16] Using similar GICs process, Milner et al. reported that potassium−ammonia solution intercalate into nanographite fibres to form nanographene platelets when dissolved in THF.[18] Conversely, alkali metal intercalated multi-walled carbon nanotubes have been shown to yield graphene ribbons through opening of the constrained tube walls[19,20]

Nano-sized graphene, with size typically smaller than 100 nm, called graphene quantum dots (GQDs),[21-28] has been synthesized or fabricated from various carbon-based materials. GQDs exhibit strong emission from blue to orange color. In recent years, graphene quantum dots have been found to have potential applications in photoluminescence (PL) detection, biomedicine and bioimaging.[28-33] All the above GQDs were fabricated using aggressive oxidation processes and the resulting GQDs were functionalized by oxygen containing functional groups. Starting from graphite nanofibres (GNFs) and using a modified Hummers' method, nanocolloidal graphene oxide[34] and graphene quantum dots[35] of ca 10 - 20 nm lateral size have been obtained. However, both are obtained using the graphene oxide route that uses strong oxidizing medium. Graphene, without oxygen passivation or functionalization, is considered non-emissive. However, as discussed in some reports, luminescence of GQDs is attributed to free zigzag sites[22,36,37] and sp^2 crystallite clusters.[21,31] As lateral size decreases down to nm scale, the concentration of free zigzag sites on nano graphene is much higher than for large lateral size graphenes. Hence, nano graphene might exhibit far more efficient photoluminescence. GQD have been obtained by sonication-aided liquid phase exfoliation of GNFs in DMSO but no PL was reported.[38]

Using mild reductive dissolution, we report here the preparation of stable, fully exfoliated, solutions of nanographenides calibrated in lateral size. Exposure of these solutions to air yields strong photoluminescence, whereas air exposure of graphenide solutions from natural graphite, performed as blank experiment, show only negligible PL.

Experimental

Materials

Graphite nanofibres (GNF)[39] were purchased from Aldrich (ref 698830, produced by catalytic chemical vapor deposition) and used as received. Raman spectra, XPS, SEM and TEM characterization of the nanofibres are presented in Figures S1-S5. NMP (Aldrich, anhydrous) was distilled under reduced pressure before entering the inert atmosphere glove box. Dry

Journal Name RSCPublishing

ARTICLE

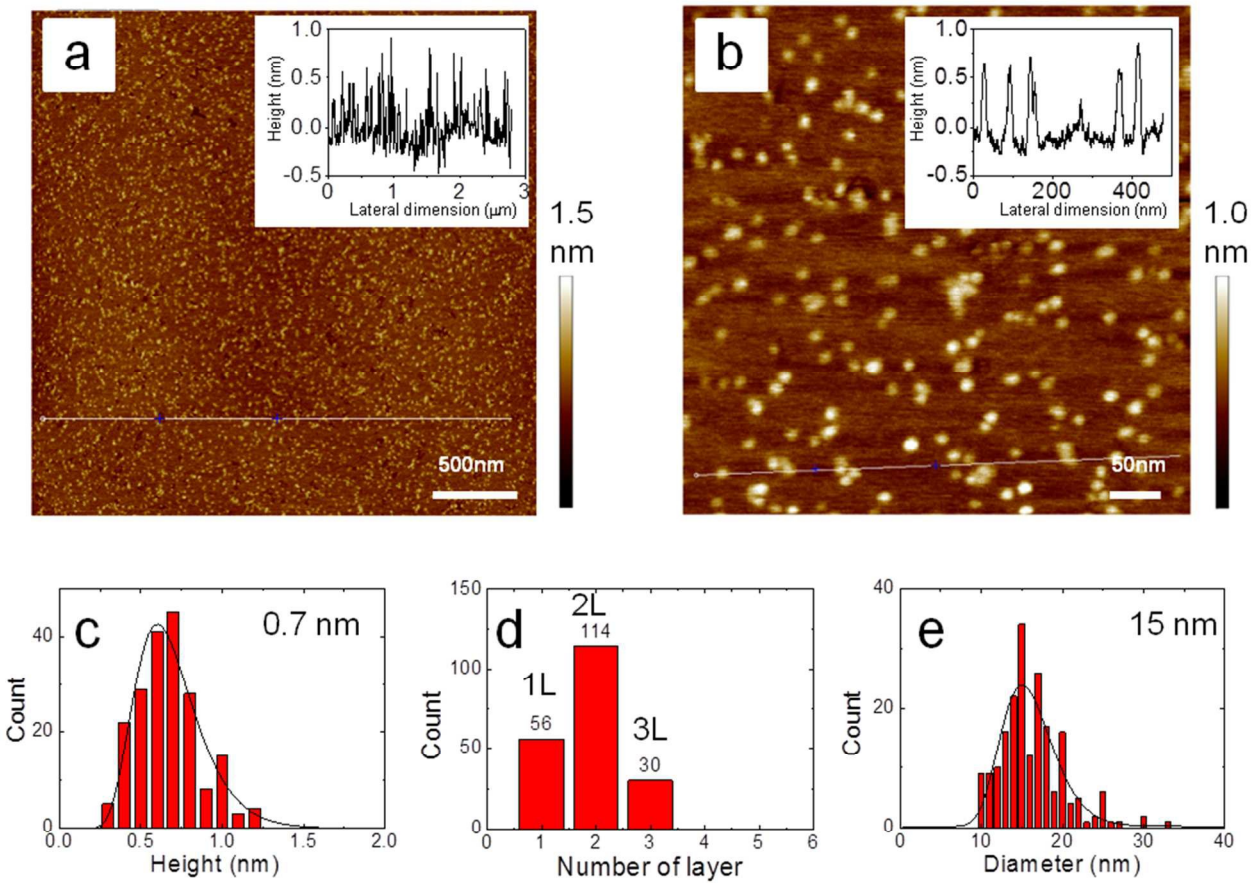

Fig. 1 (a, b) AFM topography images of deposits of GNFIC/THF solution on freshly cleaved mica surfaces. Cross sections of the topography images taken along the white line are plotted in inserted figures, showing that the height of the nano objects on the surface is less than 1 nm. (c) Height distribution of nanographene based on (b); the mean height of the objects is 0.7 nm. (d) Number of layer distribution in (b) calculated from the height distribution, assuming a height of 0.34 nm per layer and setting thresholds at 0.51 nm between 1 and 2 layers and 0.85 between 2 and 3 layers. The majority of objects have 1 or 2 layers. (e) Lateral size distribution of nanographenes based on (b); the mean size is 15 nm before tip deconvolution (see text). Lines in (c) and (e) correspond to a log normal distribution fit.[41]

THF (Aldrich, contains no stabilizer) was dried on an alumina PureSolv purifier column from Innovative Technologies and then distilled in the glove box. Surface-enhanced Raman spectroscopy (SERS) substrates, covered by Ag particles (RANDA) were purchased from Integrated Optics. Template-stripped Au surface was prepared as described in the literature.[40] All air sensitive procedures (preparation of KC_8 and its solutions, handling of the solutions, deposition on surfaces) were performed in an Innovative Technology Inc. glove box with less than one ppm O_2 and moisture contents. (Caution: Users should take extreme care when manipulating potassium and any potassium containing waste. Detailed procedures are described in Supplementary Information).

Preparation of graphite nanofibre intercalation compound (GNFIC). GNF was mixed with the appropriate amount of potassium metal (using a molar ratio C/K=8) in a sealed tube. The reaction took place at 250 ºC under vacuum. Brownish GNFIC (as compared to golden/copper shine KC_8 from graphite) was recovered after two days reaction.

Preparation of the GNFIC (KC_8) solution. About 8 mg of GNFICs were dissolved in 4 mL of distilled anhydrous THF and NMP under inert atmosphere, at room temperature using a vortex stirrer (2000 rpm). After two days, the solutions were centrifuged at 6000 rpm for 20 minutes to separate the non-soluble material from the solution. The upper clear solutions were collected into a second centrifugation tube. Then a second centrifugation was performed at the same speed of 6000 rpm for 10 minutes. After the second centrifugation, the graphenide solutions: GNFIC in THF and NMP were recovered and stored in glove box in brown vials.

Journal Name RSCPublishing

ARTICLE

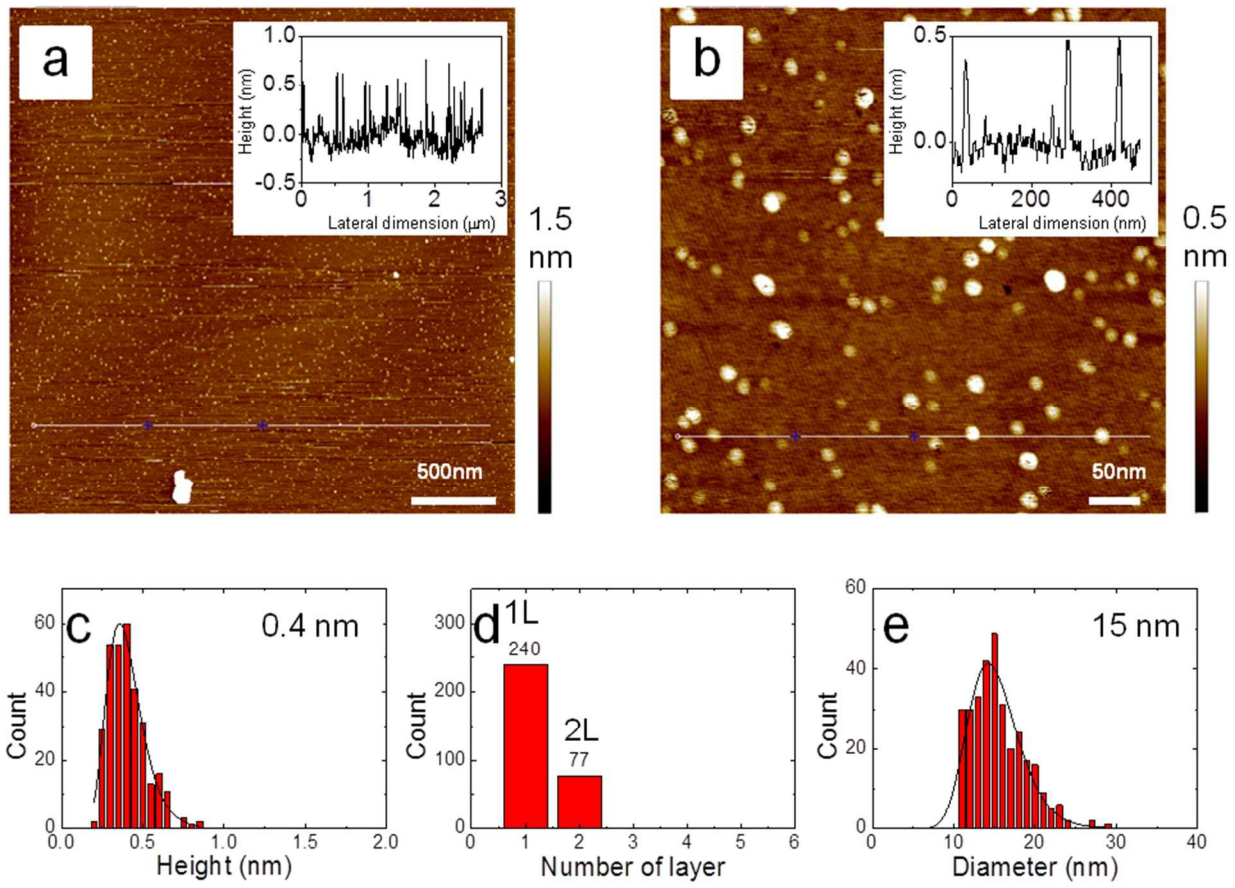

Fig. 2 (a, b) AFM topography images of deposits of GNFIC/NMP solution on freshly cleaved mica surfaces. Cross sections of the topography images taken along the white line are plotted in inserted figures, showing that the height of the nano objects on the surface is less than 1 nm. (c) Height distribution of nanographene based on (b); the mean height of the objects is 0.4 nm. (d) Number of layer distribution in (b) calculated from the height distribution, assuming a height of 0.34 nm per layer and setting thresholds at 0.51 nm between 1 and 2 layers. The majority of objects have 1 layer only. (e) Lateral size distribution of nanographenes based on (b); the mean size is 15 nm before tip deconvolution (see text). Lines in (c) and (e) correspond to a log normal distribution fit.[41]

Deposition of the solutions onto substrates. Deposits of the graphene solutions were prepared onto different kind of substrates by drop-casting inside the glove box. Deposits were performed on mica, HOPG, Au, SiO_2 and SERS surfaces. Mica and HOPG substrates were freshly cleaved in the glove box just before using. Au surfaces were separated from mica in THF[40] and washed with deionized water and ethanol, then immediately transferred into the glove box for deposition. SiO_2 surfaces were sonicated in deionized water, acetone and ethanol. SERS substrates were washed with deionized water and ethanol. For all the substrates, 30µl of graphenide solutions were deposited on ~1cm^2 substrates. The coated surfaces were dried under vacuum at room temperature and then taken out of the glove box and washed carefully using deionized water, isopropanol and deionized water. Finally, the mica and SiO_2 substrates were dried at 200°C overnight; the HOPG, Au and SERS substrates were dried at 50°C under vacuum overnight.

Atomic force microscopy (AFM). AFM images in ambient air were acquired using a Nanoscope III microscope operated in tapping mode using 8 nm radius tips MPP-111000.

Scanning tunneling microscope (STM). Ambient STM images were recorded on Nanoscope III microscope operated in STM mode using freshly cutted Platinum/Iridium tip (Pt 80/Ir 20, 0.25mm diameter).

Transmission electron microscopy (TEM). TEM images were obtained on Hitachi H7650 in Bordeaux Imaging Centre.

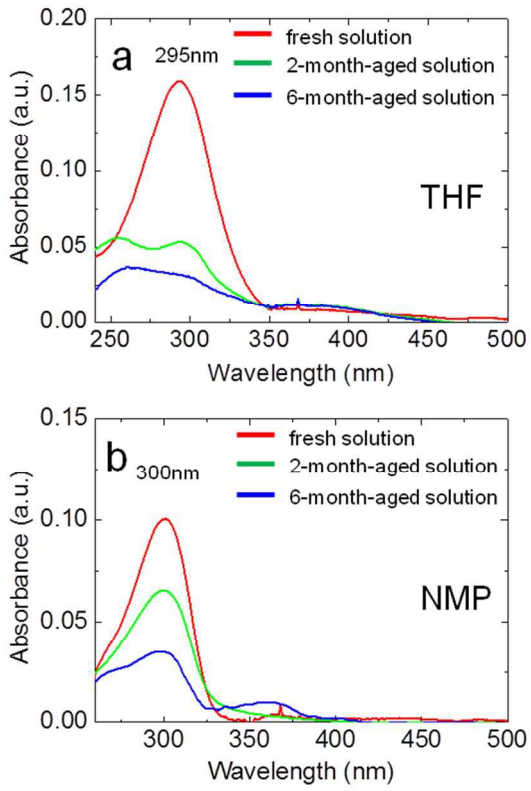

Fig. 3 Absorption spectra of (a) GNFIC/THF and (b) GNFIC/NMP. The result present the evolution process of fresh (red), 2-month-aged (green) and 6-month-aged (blue) solutions.

Raman spectroscopy. Raman spectroscopic characterization was carried out on a Horiba Jobin Yvon Xplora (excitation wavelength: 638 nm) with a laser spot size of ~1 µm. The spectra were calibrated in frequency using a piece of silicon prior to measurement. Raman mapping measurements were obtained through a motorized x-y table in a continuous linescan mode (SWIFT-module).
UV-Vis absorption spectroscopy. UV-Vis spectra were recorded on a Unicam spectrometer.
X-ray photoelectron spectroscopy (XPS). A ThermoFisher Scientific K-ALPHA spectrometer was used for surface analysis with a monochromatized AlKα source (hν = 1486.6 eV) and a 200 microns spot size. A pressure of 10^{-7} Pa was maintained in the chamber during analysis. The full spectra (0-1150 eV) were obtained with constant pass energy of 200 eV and high resolution spectra at constant pass energy of 40 eV. Charge neutralization was applied for all samples. High resolution spectra were fitted and quantified using the AVANTAGE software provided by ThermoFisher Scientific and the Scofield sensitivity factors available from the internal database. All binding energies (BEs) were referenced to Au4f or Si2p.
Photoluminescence. Photoluminescence experiments were performed using JASCO FP-8300 fluorescence spectrometer with an excitation wavelength at 325 nm.

Results and discussion

The concentration of GNFIC in THF (determined by dry extract) was between 0.2 and 0.5 mg/ml (10-30% yield from the starting material). The GNFIC solution concentrations in NMP were not determined due to NMP's high boiling point.
Upon air exposure of deposits from the graphenide solutions, re-oxidation takes place, graphenide returning mostly to neutral graphene as has been documented elsewhere[14,18] whereas oxygen gets reduced to superoxide that will eventually lead to KOH in presence of moisture. Rinsing of the surfaces allows to get rid of any potassium as XPS analysis have shown (vide infra). Nano-sized graphenes were adsorbed on atomically smooth mica surfaces from THF or NMP solutions to explore their morphology. Examination of the topography image (Fig. 1a-b) of GNFIC/THF deposition on mica reveals a very flat surface, bearing homogenous nano-objects characterized by a height less than 1 nm (see full sized cross section in the inset). Single objects can be clearly observed with height around 0.4-0.8 nm and width around ~15 nm in Fig. 1b. These objects are identified as nano graphenes, since their height falls in the expected size range of mono- or bi-layer graphene. Statistical analysis of the height distribution (Fig. 1c) gives a mean height of 0.7 nm for the nano graphenes which agrees well with bilayer graphene thickness. Converting the height distribution into number of layers as shown in Fig. 1d, we found that ca 85% of the objects are single- and bi-layer nano graphene. The statistical analysis of diameter distribution (Fig. 1e) shows a monodisperse lateral size of ca 15 nm with a narrow distribution. The lateral size of nanographene was calculated as ca 10 nm considering the tip convolution effect of 8 nm ultra-sharp AFM tip used.
Similar results were founded from the images of GNFIC/NMP deposition on mica (Fig. 2). From the images and the corresponding cross sections, the heights of almost all the objects are lower than 0.5 nm. Height distribution gives a mean height of 0.4 nm. Only monolayer and bilayer nano graphenes were found in Fig. 2d and the percentage of single layer reaches 76%.
The UV-Vis spectra (Fig. 3) of GNFIC/THF and GNFIC/NMP show one absorption band at ~300 nm in both fresh solutions, associated to charged graphene (graphenide) in solution.[14] The solutions were stored under inert atmosphere and examined again after 2 and 6 months. The UV-Vis spectra of these aged solutions are also shown in Fig. 3. For GNFIC/THF solution (Fig. 3a), the intensity of the 300 nm band was dramatically decreased for the 2-month-aged solution and full disappearance was observed after 6 months of storage, while a new small band appears at 260 nm. A similar but less pronounced tendency was observed for the GNFIC/NMP solution (Fig. 3b).
Due to the small size of nano graphene, Raman signals of the deposits from GNFIC solutions in THF and NMP were very weak and no clear graphitic peaks could be identified. To get an enhanced Raman signal, the GNFIC/THF and GNFIC/NMP fresh and 6-month-aged solutions were deposited on SERS substrates and Raman mapping was recorded (Fig. 4). Representative Raman spectra of GNFIC fresh solutions and 6-month-aged solutions in THF and NMP are shown in Fig. 4a and 4b. The G band (1590 cm^{-1}), 2D band (2646 cm^{-1}) and an intense D band (1346 cm^{-1}) as expected due to edge effects of graphite nanofibres, are clearly visible in all cases. Statistical analysis of the I_D/I_G ratio extracted from the Raman mapping is presented in

Journal Name RSCPublishing

ARTICLE

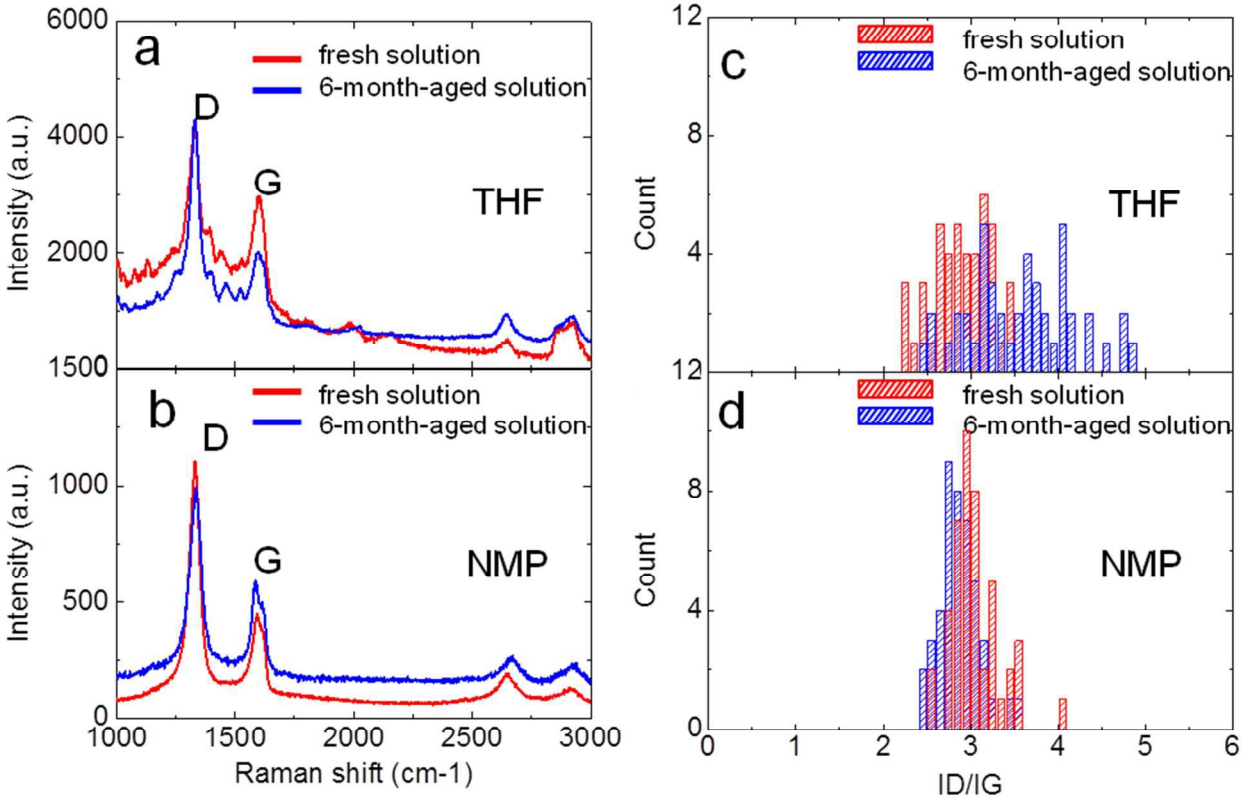

Fig. 4 Representative SERS Raman spectra of GNFIC in (a) THF and (b) NMP. Both fresh (red curve) and 6-month-aged (blue curve) solution depositions on SERS surfaces are presented. (c) The ID/IG ratio of GNFIC in THF increases when solutions age. (d) The ID/IG ratio of GNFIC in NMP remains constant even for aged solutions.

Fig. 4c and 4d. The I_D/I_G ratios of GNFIC fresh solutions in THF and NMP are 3 and 2.9 respectively with a narrow distribution very close to the value of 2.8 for the starting graphite nanofibre. This suggests that the whole exfoliation procedure does not induce additional defects on the nano graphene. Using Cançado's equation,[42] the crystallite size of nanographene, L_a can be calculated from I_D/I_G ratio. For GNFIC fresh solutions in THF and NMP, the crystallite sizes are around 14 nm which is quite close to the 10 nm diameter observed by AFM. The I_D/I_G ratio of GNFIC/THF 6-month-aged solution has, in turn, a mean value at 3.8 with a very broad distribution, while that of GNFIC/NMP 6-month-aged solution remains at 2.9. The increase and broader distribution of the I_D/I_G ratio of aged GNFIC/THF solution evidences its evolution. On the contrary, the unchanged I_D/I_G ratio of aged GNFIC/NMP solution supports the idea of stable GNFIC/NMP solutions.

Additionally, transmission electronic microscopy (TEM) observation of GNFIC/NMP fresh solution deposited on carbon film/copper grids shows a similar statistical diameter distribution with an average lateral size of 12 nm (Fig. 5a-b). Ambient scanning tunneling microscopy (STM) experiment also recorded for deposits from GNFIC/NMP fresh solution on HOPG, showed many nano graphene flakes and a lateral size range from 10 to 30 nm (Fig. 5c). A high resolution STM image (Fig. 5d) shows one nano graphene flake. The cross section (insert figure) shows a height difference of ca 0.4 nm between substrate and nano graphene. Higher spots are found mainly on the edges with typical heights from 0.5 to 1.5 nm.

The small lateral size of the nanographene deposits obtained from GNF starting fibres with a wide distribution of diameters is puzzling. Characterization of deposits for different intercalation and dissolution times showed no variation on size, ruling out a kinetic effect. Microscopy examination of the GNF starting fibres shows that small diameter GNF fibres are clearly seen in TEM images (see Fig. S2 and S3 in SI), consistent with the ca 10 nm lateral size of nano graphene after exfoliation. We hypothetize that smaller GNF fibres are more easily exfoliated than larger nanofibres, probably because they have less (or no) interbonds between graphite layers. Three other sources of GNF nanofibres starting materials were also studied using

Journal Name RSCPublishing

ARTICLE

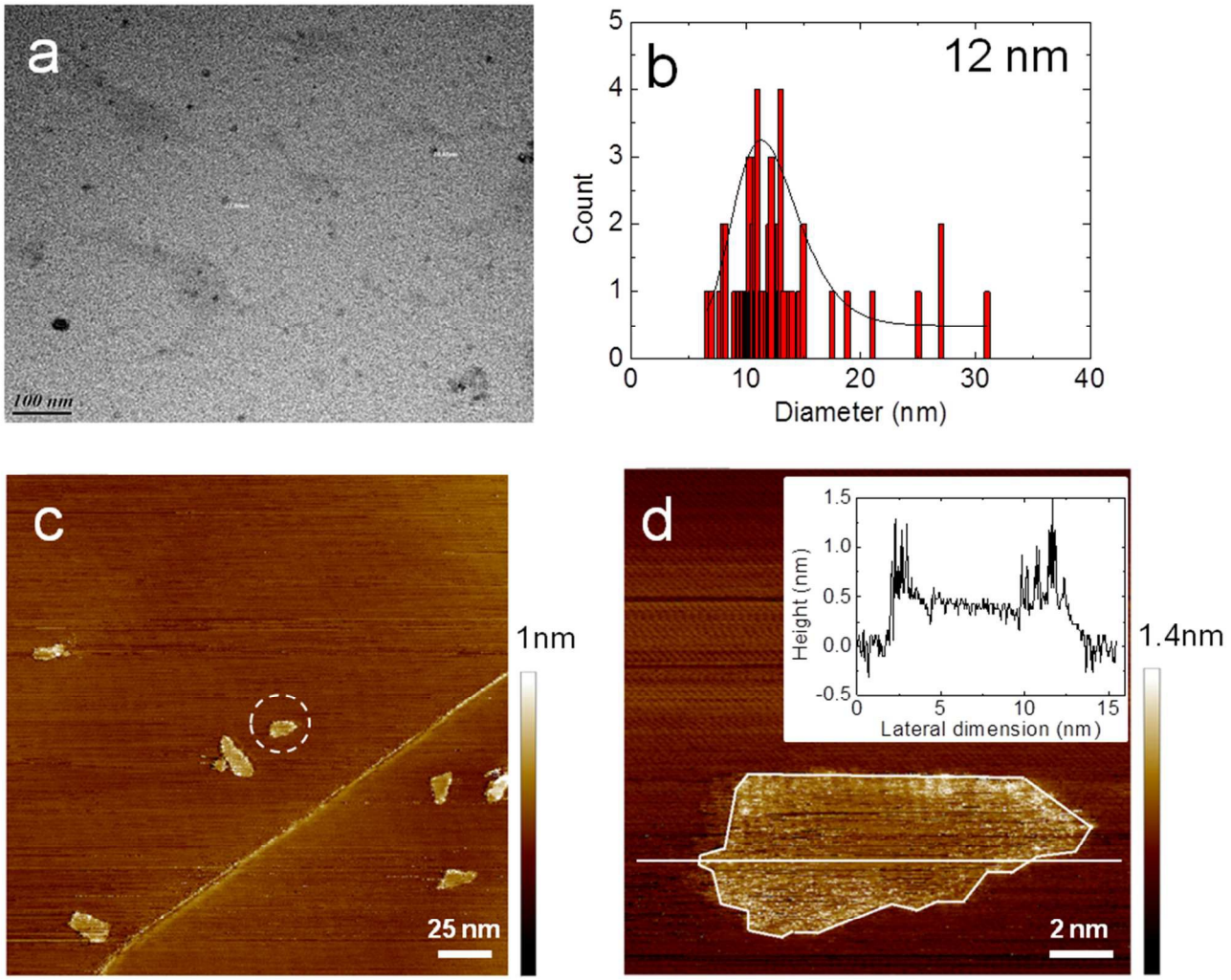

Fig. 5 (a) TEM image of deposits of GNFIC/NMP fresh solution on carbon film/copper grids. (b) Lateral size statistic analysis of nano graphene in (a) shows a mean size of 12 nm. Line in (b) corresponds to a log normal distribution fit.[41] (c) Ambient STM image (V_{bias} = -100 mV, I_t = 0.25 nA) of a deposit of GNFIC/NMP fresh solution on HOPG. (d) High resolution ambient STM image (V_{bias} = -100 mV, I_t = 0.2 nA) on a single nano graphene (circled region in c). Inset: Cross-section measured along the white line, showing that the height of the nano graphene is ca 0.4 nm. See the discussion in text.

AFM and SERS Raman and similar results were obtained (see SI, Figures S8-11 for detailed information).

XPS spectra were recorded on the deposits of GNFIC/THF fresh and aged solutions on Au surfaces treated at 50°C under vacuum. In order to be able to remove absorbed NMP solvent, SiO_2 substrates were used for the deposition of GNFIC/NMP solutions and treated at 200°C overnight. Starting GNF nanofibres were also dispersed in ethanol by weak sonication and deposited on Au and SiO_2 surfaces and followed by the same treatment. The C1s core-level signals obtained on these surfaces are shown in Fig. 6 (see Fig. S6 in SI for the detailed fitting). Both fresh and aged GNFIC/THF C1s signals (Fig. 6a) show a peak at 284.6 eV while the C1s signal of starting GNF nanofibre shows a peak at 284.2 eV. This shift could be explained by a strong interaction (or doping effect) between graphene and Au. This interaction also results in a small increase of the FWHM (1.24 eV) for GNFIC/THF compared with GNF nanofibres (1.05 eV). In the case of GNF nanofibres, the collected photoelectrons only give the information of stacked graphite nanofibres without any interference of the substrate: the 10 nm XPS signal depth is smaller than the GNF diameter. On the contrary, for the GNFIC depositions, both the information of the graphene flakes (mono- or bi-

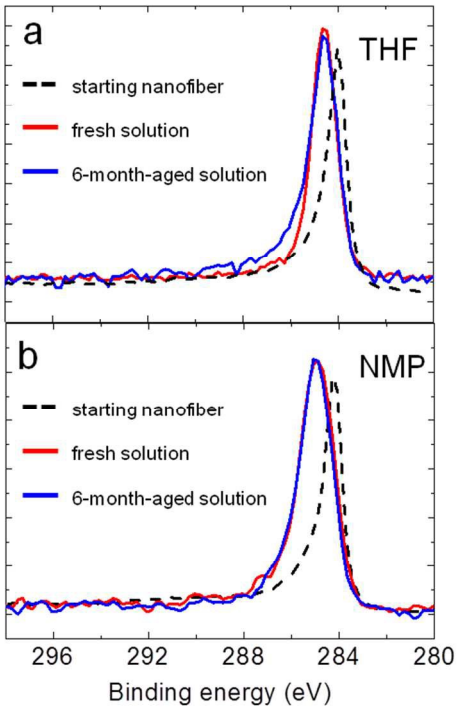

Fig. 6 (a) Core-level C1s XPS spectra of GNFIC/THF solution deposited on Au surface and (b) GNFIC/NMP solution deposited on SiO_2 surface. The result of starting nanofibre presented in black curve.

layer, less than 1 nm) and the information of the interaction between graphene and the surface are detected by XPS. The aged GNFIC/THF shows a broader C1s peak with a more intense higher binding energy tail. This is attributed to C-O, C=O and COO contributions[43] caused by the graphene oxidation or functionalization in aged GNFIC/THF solution. For both depositions of fresh and aged GNFIC/NMP on SiO_2 substrate, the C1s peaks are found at 284.8 eV. This larger shift (0.7 eV) suggests a stronger interaction between graphene and SiO_2 compared with Au (in the case of GNFIC/THF on Au, the shift was about 0.4 eV) which agrees with the literature.[44] More importantly, almost the same shape for the C1s signal and no increase at higher binding energy are observed for fresh and aged GNFIC/NMP solutions. This suggests that neither carbon-oxygen bonds nor additional defects from oxidation or functionalization on the graphene were created in aged GNFIC/NMP solutions. The XPS result of fresh and aged GNFIC/THF and GNFIC/NMP solutions provide further evidence on solution stability.

Fig. 7a displays photoluminescence spectra of a GNFIC/NMP sample upon air exposure from t=0 (before opening) to t~42h. The appearance of a broad PL line when the sample is exposed to air can be observed. However, air exposure of graphenide solution from natural graphite shows only negligible PL (see Fig. S7 in SI). The intensity of the PL line continuously increases during several hours. Moreover, the maximum of the line shifts to the red (~35 nm) at almost the same time scale. This PL signal is probably due to edge states that are created by exposing the graphenide compounds to air. Fig. 7b shows both the intensity and the position of the line as a function of time.

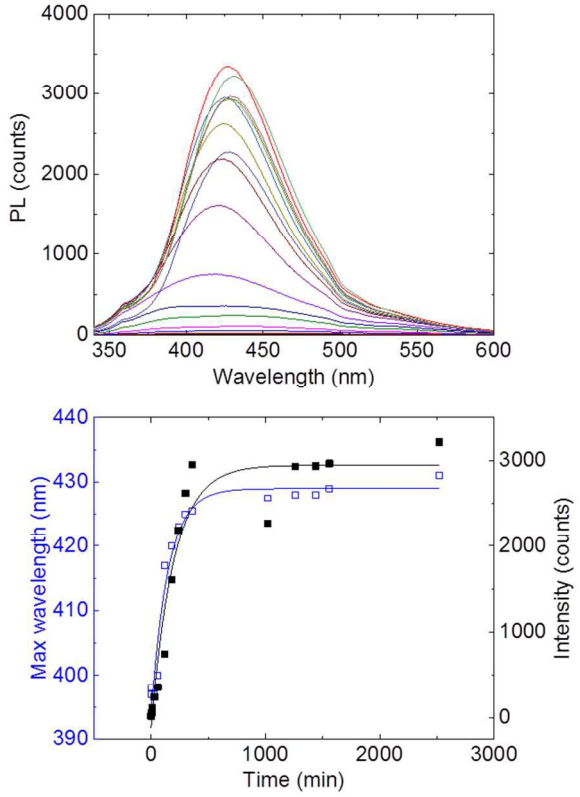

Fig. 7 (a) Photoluminescence spectra of the GNFIC/NMP fresh solution from t=0 (before opening) to t~42h. (b) PL peak position (blue open square) and peak intensity (black solid square) as a function of time. Straight lines are fits with a first order reaction (see text).

Let us first consider the variation of the intensity. One observes both an increase and a saturation of the PL intensity as a function of time. This saturation curve can be well-fitted by considering a pseudo-first order kinetic reaction. If we consider the chemical reaction $[G]_{red} + [O_2] \rightarrow [G]_{edge}$ with $[G]_{red}$ the concentration of graphenide species, $[O_2]$ the oxygen and $[G]_{edge}$ the concentration of edge states that emit light. As the oxygen reservoir can be considered infinite, the pseudo-monomolecular reaction will satisfy $d[G]_{edge}/dt = k'[G]_{red}$, with k' the monomolecular velocity constant, and the concentration of oxidized edge states will grow as $1\text{-}exp(-k't)$. The black curve in Fig. 7b is a fit of the data with this model; a good agreement between the data and the fit can be observed. Finally, a saturation of the red shift of the PL signal is also observed (blue curve in Fig. 7b). The global red shift may have several origins. Among them, if the line is inhomogeneously broadened due to a wide energy distribution of emitting states differing from one platelet to the other, the red shift can account for a change in the distribution with an increasing weight for the low energy states during the chemical reaction. However, Xu et al have demonstrated that the PL of one single nano graphene platelet has the same line shape than the one obtained on an ensemble measurements, i.e. a broad emission line in the UV-Vis.[45] This paper demonstrates that the broad linewidth of such PL signal is not due to

dispersion of behaviour from one platelets to the other. Another origin of the red shift may be related to a coupling between the edge states along the chemical reaction. Indeed, such coupling could lead to a delocalization of the electrons, and the longer is the delocalization, the lower is the energy of the emitting state. In order to test this hypothesis, life time measurements during the exposition to air are planned.

Conclusions

Graphite nanofibres can be fully exfoliated by using graphite intercalation compounds (GICs) process. We obtained nano-sized single layer graphene platelets in THF and NMP. AFM analysis showed that the single layer nanographene platelets have an average thickness of 0.4 nm and a lateral size of 10 nm. The nanographene solution in NMP was shown to have longer stability (over 6 months) by detailed studies using SERS, UV-Vis and XPS. Upon exposure to air, the nanographene solution exhibits strong photoluminescence. The intensity increment and red-shift of the PL line indicates that the photoluminescense originates mainly from the oxidation of the edge states and the coupling among them.

Acknowledgements

Financial support from LINDE Nanomaterials USA is acknowledged. We acknowledge C. Labrugère for XPS experiments and discussion. This work has been done within the framework of the GDR-I 3217 ‘‘graphene and nanotubes’’.

Notes and references

[a] CNRS, Centre de Recherche Paul Pascal (CRPP), UPR 8641, F-33600 Pessac, France.
[b] Université Bordeaux, CRPP, UPR 8641, F-33600 Pessac, France
[c] Laboratoire Aimé Cotton, CNRS, ENS Cachan, Université Paris Sud, campus d'Orsay, bât 505 91405 Orsay cedex France.
E-mail: penicaud@crpp-bordeaux.cnrs.fr

Electronic Supplementary Information (ESI) available: [Raman, SEM, TEM and XPS characterization of the raw nanofibres, detailed XPS spectra analysis of deposits from GNFIC/THF and GNFIC/NMP solutions, Raman and AFM characterization of fresh and aged solutions of nanofibres obtained from 3 different suppliers]. See DOI: 10.1039/b000000x/

1 K. S. Novoselov, A. K. Geim, S. V. Morozov, D. Jiang, Y. Zhang, S. V. Dubonos, I. V. Grigorieva, A. A. Firsov, *Science,* 2004, **306**, 666.
2 A. K. Geim, K. S. Novoselov, *Nature Mater*., 2007, **6**, 183.
3 M. J. Allen, V. C. Tung, R. B. Kaner, *Chem. Rev*., 2010, **110**, 132.
4 S. Park, R. S. Ruoff, *Nature Nanotech*., 2009, **4**, 217.
5 W. Cai, A. L. Moore, Y. Zhu, X. Li, S. Chen, L. Shi, R. S. Ruoff, *Nano Lett*., 2010, **10**, 1645.
6 X. Li, W. Cai, J. An, S. Kim, J. Nah, D. Yang, R. Piner, A. Velamakanni, I. Jung, E. Tutuc, S. K. Banerjee, L. Colombo, R. S. Ruoff, *Science*, 2009, **324**, 1312.
7 C. Berger, Z. Song, T. Li, X. Li, A. Y. Ogbazghi, R. Feng, Z. Dai, A. N. Marchenkov, E. H. Conrad, P. N. First, W. A. de Heer, *J. Phys. Chem. B,* 2004, **108**, 19912.
8 Y. Hernandez, V. Nicolosi, M. Lotya, F. M. Blighe, Z. Sun, S. De, I. T. McGovern, B. Holland, M. Byrne, Y. K. Gun'Ko, J. J. Boland, P. Niraj, G. Duesberg, S. Krishnamurthy, R. Goodhue, J. Hutchison, V. Scardaci, A. C. Ferrari, J. N. Coleman, *Nature Nanotech.*, 2008, **3**, 563.
9 W. Qian, R. Hao, Y. Hou, Y. Tian, C. Shen, H. Gao, X. Liang, *Nano Res.*, 2009, **2**, 706.
10 S. Malik, A. Vijayaraghavan, R. Erni, K. Ariga, I. Khalakhan, J. P. Hill, *Nanoscale,* 2010, **2**, 2139.
11 A. B. Bourlinos, V. Georgakilas, R. Zboril, T. A. Steriotis, A. K. Stubos, *Small,* 2009, **5**, 1841.
12 X. An, T. Simmons, R. Shah, C. Wolfe, K. M. Lewis, M. Washington, S. K. Nayak, S. Talapatra, S. Kar, *Nano Lett.*, 2010, **10**, 4295.
13 C. Valles, C. Drummond, H. Saadaoui, C. A. Furtado, M. He, O. Roubeau, L. Ortolani, M. Monthioux, A. Penicaud, *J. Am. Chem. Soc.*, 2008, **130**, 15802.
14 A. Catheline, C. Valles, C. Drummond, L. Ortolani, V. Morandi, M. Marcaccio, M. Iurlo, F. Paolucci, A. Penicaud, *Chem. Commun.*, 2011, **47**, 5470.
15 A. Catheline, L. Ortolani, V. Morandi, C. Drummond, C. Zakri, A. Penicaud, *Soft Matter*, 2012, **8**, 3882.
16 A. Penicaud, C. Drummond, *Acc. Chem. Res.*, 2013, **46**, 129.
17 D. Voiry, C. Drummond, A. Penicaud, *Soft Matter*, 2011, **7**, 7998.
18 E. M. Milner, N. T. Skipper, C. A. Howard, M. S. P. Shaffer, D. J. Buckley, K. A. Rahnejat, P. L. Cullen, R. K. Heenan, P. Lindner, R. Schweins, *J. Am. Chem. Soc*., 2012, **134**, 8302.
19 D. V. Kosynkin, W. Lu, A. Sinitskii, G. Pera, Z. Sun, J. M. Tour, *ACS Nano*, 2011, **5**, 968.
20 A. G. Cano-Marquez, F. J. Rodriguez-Macias, J. Campos-Delgado, C. G. Espinosa-Gonzalez, F. Tristan-Lopez, D. Ramirez-Gonzalez, D. A. Cullen, D. J. Smith, M. Terrones, Y. I. Vega-Cantu, *Nano Lett*., 2009, **9**, 1527.
21 G. Eda, Y. Lin, C. Mattevi, H. Yamaguchi, H. Chen, I. Chen, C. Chen, M. Chhowalla, *Adv. Mater.*, 2010, **22**, 505.
22 D. Pan, J. Zhang, Z. Li, M. Wu, *Adv. Mater.*, 2010, **22**, 734.
23 S. Kim, S. Hwang, M. Kim, D. Shin, D. Shin, C. Kim, S. Yang, J. Park, E. Hwang, S. Choi, G. Ko, S. Sim, C. Sone, H. Choi, S. Bae, B. Hong, *ACS Nano*, 2012, **6**, 8203.
24 F. Liu, M. Jang, H. Ha, J. Kim, Y. Cho, T. Seo, *Adv. Mater.*, 2013, **25**, 3657.
25 Y. Sun, S. Wang, C. Li, P. Luo, L. Tao, Y. Wei, G. Shi, *Phys. Chem. Chem. Phys.*, 2013, **15**, 9907.
26 L. Li, G. Wu, G. Yang, J. Peng, J. Zhao, J. Zhu, *Nanoscale*, 2013, **5**, 4015.
27 D. B. Shinde, V. K. Pillai, *Chem. Eur. J.*, 2012, **18**, 12522.
28 J. Peng, W. Gao, B. K. Gupta, Z. Liu, R. Romero-Aburto, L. Ge, L. Song, L. B. Alemany, X. Zhan, G. Gao, S. A.

Vithayathil, B. A. Kaipparettu, A. A. Marti, T. Hayashi, J. Zhu, P. M. Ajayan, *Nano Lett.*, 2012, **12**, 844.
29 Z. Liu, J. T. Robinson, X. M. Sun, H. J. Dai, *J. Am. Chem. Soc.*, 2008, **130**, 10876.
30 X. Wang, R. Lei, H. Huang, N. Wang, L. Yuan, R. Xiao, L. Bai, X. Li, L. Li, X. Yang, *Nanoscale*, 2015, **7**, 2034.
31 S. Zhu, J. Zhang, C. Qiao, S. Tang, Y. Li, W. Yuan, B. Li, L. Tian, F. Liu, R. Hu, H. Gao, H. Wei, H. Zhang, H. Sun, B. Yang, *Chem. Commun.*, 2011, **47**, 6858.
32 B. Tian, C. Wang, S. Zhang, L. Feng, Z. Liu, *ACS Nano*, 2011, **5**, 7000.
33 L. Lin, S. Zhang, *Chem. Commun*., 2012, **48**, 10177.
34 J. Luo, L. J. Cote, V. C. Tung, A. T. L. Tan, P. E. Goins, J. Wu, J. Huang, *J. Am. Chem. Soc.*, 2010, **132**, 17667.
35 S. Abdul Rashid, S. A. Mohd Zobir, S. Krishnan, M. M. Hassan, H. N. Lim, *J. Nanoparticle Res.*, 2015, **17**, 225.
36 V. Gupta, N. Chaudhary, R. Srivastava, G. D. Sharma, R. Bhardwaj, S. Chand, *J. Am. Chem. Soc.*, 2011, **133**, 9960.
37 K. A. Ritter, J. W. Lyding, *Nature Mater.*, 2009, **8**, 235.
38 Y.-W. Shih, G.-W. Tseng, C.-Y. Hsieh, Y.-Y. Li, and A. Sakoda, *Acta Mater.*, 2014, **78**, 314.
39 N. M. Rodriguez, A. Chambers, and R. T. K. Baker, *Langmuir*, 1995, **11**, 3862.
40 M. Hegner, P. Wagner, G. Semenza, *Surf. Sci*. 1993, **291**, 39.
41 E. Limpert, W. A. Stahel, M. Abbt, *Bioscience*, 2001, **51**, 341.
42 L. G. Cancado, K. Takai, T. Enoki, M. Endo, Y. A. Kim, H. Mizusaki, A. Jorio, L. N. Coelho, R. Magalhaes-Paniago, M. A. Pimenta, *Appl. Phys. Lett*., 2006, **88**, 163106.
43 H. Shin, K. Kim, A. Benayad, S. Yoon, H. Park, I. Jung, M. Jin, H. Jeong, J. Kim, J. Choi, Y. Lee, *Adv. Funct. Mater*. 2009, **19**, 1987.
44 S. Ryu, L. Liu, S. Berciaud, Y.-J. Yu, H. Liu, P. Kim, G. W. Flynn, L. E. Brus, *Nano Lett.*, 2010, **10**, 4944.
45 Q. Xu, Q. Zhou, Z. Hua, Q. Xue, C. Zhang, X. Wang, D. Pan, M. Xiao, *ACS Nano*, 2013, **7**, 10654.